Exergy-based fault detection on the Tennessee Eastman process

J. Vosloo [*] **K.R. Uren** [*] **G. van Schoor** [**] **L. Auret** [***]
H. Marais [*]

[*] *School of Electrical, Electronic, and Computer Engineering, Faculty of Engineering, North-West University, South Africa. (e-mail: johandri.vosloo@gmail.com; kenny.uren@nwu.ac.za)*
[**] *Unit for Energy and Technology Systems, Faculty of Engineering, North-West University, South Africa (e-mail: george.vanschoor@nwu.ac.za)*
[***] *School of Process Engineering, Stellenbosch University, South Africa (e-mail: lauret@sun.ac.za)*

Abstract: The exergy-based fault detection method has not yet been applied to a complex industrial system that adequately represents a dynamically changing process. One such system, the Tennessee Eastman process, is commonly used as a benchmark for fault detection methods. In this paper, an exergy-based fault detection approach is applied to the Tennessee Eastman process. This is done to investigate the feasibility of using this approach when confronted with noisy sensor data and control loops masking faulty behaviour. An exergy characterisation was performed on stream data obtained from the Tennessee Eastman process. The exergy characterisation included a new approach to calculate the standard chemical exergy of unknown components. For fault detection, threshold limits were determined for the exergy characterisation when normal operating conditions are assumed. The threshold limits were calculated following the upper and lower control limit determination of the Shewhart control chart. The results showed that this method could quantify both the physical state as well as the chemical features of the process and that 17 out of the 20 considered faults could be detected. This shows that the exergy-based method could be adequately applied to the Tennessee Eastman process.

Keywords: Fault detection; Exergy; Tennessee Eastman process

1. INTRODUCTION

In modern industrial processes, great importance is placed on producing high-quality products, with minimal process downtime while also maintaining the highest standard of operational safety. Any malfunction of process equipment or deviations from normal operating conditions can significantly increase manufacturing costs and influence product quality. Not to mention the risks such deviations can pose to process safety and its impact on the surrounding environment. Driven by the need to prevent most, if not all, process malfunctions, process monitoring and fault diagnosis have received significant attention in recent years and continues to be a growing field of interest (Ammiche et al., 2018; Chen et al., 2016; Reis and Gins, 2017).

The difficulty with which fault diagnosis can be performed depends considerably on the nature of the fault. Total breakdown of a piece of equipment can be relatively easy to detect, however by the time of occurrence, irreparable damage could have already occurred. Detection of incipient or latent failures can be more problematic. Due to the interaction between process components in complex systems, it has been found to be very difficult to distinguish between the faults' causes and their inevitable effects. The complexity

of the process ensures that when a fault occurs in one part of the system, it can propagate throughout the rest of the system. Complex industrial processes therefore call for interpretable fault detection and diagnosis methods that can accurately detect and evaluate the type of fault as well as ascertain its root cause (Ragab et al., 2018; Wang et al., 2018).

Through the years a wide variety of methods and approaches have been proposed, all of which varies in their feasibility and effectiveness for fault detection and diagnosis. All these methods can be classified as either model-based or data-driven. (Bouamama et al., 2014; Venkatasubramanian et al., 2003b). In model-based fault detection, it is assumed that there is prior knowledge about the model of the process and the model is constructed using some fundamental knowledge of the physics of the process. In contrast to this, data-driven methods assume the availability of a great amount of historical process data (Eslamloueyan, 2011; Venkatasubramanian et al., 2003b). If possible, fault detection should be quick and easy, however, due to the presence of model uncertainties, process noise, disturbances in the process and its environment, this task can become difficult. This, in turn, could delay the detection and isolation of faults as well as lead to

incorrect diagnosis (Bouamama et al., 2014). Developing a robust method that can accurately detect and diagnose faults even in the presence of uncertainties and noise is therefore of key importance.

In recent years, with the advancements in computer control and artificial intelligence, data-driven methods have become more popular, especially applied to those complex processes where model-based methods are almost impossible to construct (Ge et al., 2013; Guo and Kang, 2015). Data-driven methods require a pre-processing step that extracts valuable information from the available data, so its performance is highly reliant on the quantity and quality of the processed data. As a result, any lack of suitable data can compromise its diagnostic abilities (Bouamama et al., 2014; Tidriri et al., 2018b). Unfortunately, it is still extremely challenging to determine the root cause of a fault by using just data-driven methods, especially when considering complex industrial processes where recycle loops and elaborate process control are prevalent (Ge et al., 2013; Guo and Kang, 2015).

While both methods have their various advantages and disadvantages, no single approach possesses all the desirable characteristics for the ideal diagnostic system, with their individual shortcomings being serious enough to render these methods unsuitable for use within complex industrial situations. However, if methods with complementary features are combined to develop a hybrid system, the limitations of individual methods can be overcome (Amin et al., 2018; Venkatasubramanian et al., 2003a). Subsequently, more studies are now investigating the advantages of implementing hybrid systems to bridge the gap between data-driven and model-based methods (Amin et al., 2018; Guo and Kang, 2015; Liao and Köttig, 2016; Tidriri et al., 2018b).

Marais et al. (2019) first suggested that exergy-data could be of value when used for fault diagnosis. They made use of physical and chemical exergy to calculate the total exergy of process streams present in a simulated auto-thermal reformer. The calculated exergy could describe both the physical state as well as the chemical features of the process, enabling it to quantify both changes in physical properties and chemical features. The study showed that the exergy-based approach could effectively isolate faults and it was suggested that the exergy-based method could be useful in the development of a hybrid fault diagnosis system for a complex industrial plant. This was further investigated by Greyling et al. (2019), who applied an exergy-based fault detection method to a gas-to-liquids process simulated in Aspen Hysys^{TM}. Their results showed complete detection and isolation of all considered process faults, indicating that the exergy-based method could be successfully used for a more complex system. Both of these studies utilised a basic threshold function to indicate whether the exergy values of the fault data increased or decreased from the normal operating data. The studies only considered one sample of steady-state data when using this threshold function. A dynamically changing environment would better represent a complex industrial process, however this threshold function cannot be adequately applied to dynamically changing data since

it is expected to change over a period of time, irrespective of a fault being present or not.

The purpose of this study is to show if, and how, the exergy-based fault detection method can be applied to a more realistic representation of an industrial process, i.e. a dynamically changing process that has noise and control that masks any faults that occur. The contribution of this work is to demonstrate the applicability of an exergy-based approach to fault detection. This approach will be applied to a widely used benchmark process for fault detection and diagnosis, i.e. the Tennessee Eastman process (TEP), which in turn will allow for future comparative studies. A brief description of the TEP along with its implementation is given in Section 2. How exergy is characterised and calculated is detailed in Section 3. The proposed exergy-based fault detection approach as applied to the TEP is given in Section 4, and the discussion of the results are provided in Section 5. Finally, concluding remarks are presented in Section 6.

2. TENNESSEE EASTMAN PROCESS

The TEP consists of two simultaneous gas-liquid exothermic irreversible reactions producing two products and two additional reactions producing a by-product. The process consists of five major unit operations, which include a two-phase reactor, a product condenser, a vapour-liquid separator, a recycle compressor and a product stripper, as shown by the process diagram in Fig. 1. The process has 12 manipulated variables and 41 measurements which can be used for monitoring and control. Also specified for the process are four setpoint changes, 20 different disturbances and several process constraints primarily introduced for equipment protection (Downs and Vogel, 1993).

Since its introduction, the TEP simulation has been widely used as a benchmark problem for evaluating fault detection and diagnosis methods. The results from these publications showed limitations with the fault diagnosis methods, which include the non-detectability of some faults, the assumption that multiple faults do not occur simultaneously, as well as uncertainties within the TEP such as model errors and unidentified disturbances (Maurya et al., 2007; Tidriri et al., 2018a; Yin et al., 2012). With the advancements in computer control and artificial intelligence, data-driven methods applied to the TEP have become more popular. These recent studies have shown higher detection rates as compared to other methods in literature (Ragab et al., 2018; Wu and Zhao, 2018). Although these data driven methods have shown improvements, more studies are now investigating the advantages of implementing hybrid methods for even better fault detection. Recent studies associated with hybrid techniques implemented on the TEP, show better diagnostic performance over its single method counterparts (Amin et al., 2018; Tidriri et al., 2018b). Investigating the applicability of exergy-based fault detection methods on the TEP is therefore well justified, especially as a starting point in developing an exergy-based hybrid fault detection approach. .

For the purpose of this study, the TEP was simulated using Simulink. The original FORTRAN code provided
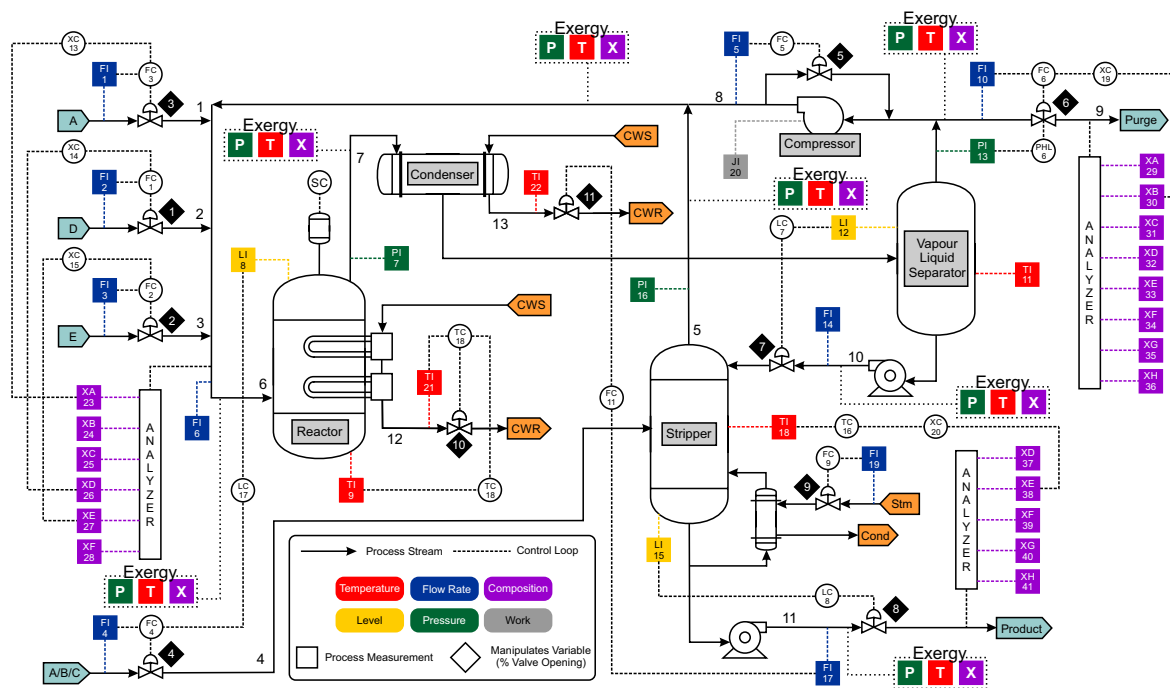
Fig. 1. Process diagram of the TEP (adapted from Downs and Vogel (1993) and Chiang et al. (2000)).

by Downs and Vogel (1993) was used to construct the process in Simulink. The TEP is controlled with the approach suggested by Lyman and Georgakis (1995), which can be seen in Fig. 1, and the controller parameters listed by Chiang et al. (2000). The sampling interval was taken as 180 s, to account for imperfection in the sensor measurements.

The TEP open-loop simulation was validated using data obtained from the original FORTRAN source code of Downs and Vogel (1993). The process measurements and manipulated variables were compared with data obtained from running the TEP Simulink model using steady-state values as initial conditions. Further validation of the Simulink model was conducted by comparing the results obtained from the closed-loop simulation of the TEP in Simulink to those found when simulating it with the FORTRAN code provided by Chiang et al. (2000). Both comparisons showed good correlation between the original FORTRAN results and those obtained from the Simulink model.

In the TEP there are 20 programmed faults. Faults 1 to 7 are related to step changes implemented in their respective process variables. Faults 8 to 12 are related to random variation in their respective process variables. Fault 13 is associated with the process reactions and imitates a slow drift within the reaction kinetics. Faults 14 and 15 represent sticking valves. Faults 16 to 20 are unknown. For further detail on these faults see Downs and Vogel (1993).

3. EXERGY CHARACTERISATION

Any industrial process plant can be described as a series of matter and energy exchanges to attain the desired product. These exchanges can transpire within any physical domain which includes, but are not limited to

the chemical, thermal, electrical and mechanical domains. Across all these physical domains, energy can be defined as the unifying concept to portray the relevant characteristics of the industrial process. From this, a complex process plant can be characterised by a set of energy parameters that hold structural relation to the physical system. The advantage of using exergy is that it provides a method with which to quantify the quality of an energy stream. This is because exergy can simply be defined as the amount of energy available for use (Brockett, 2017).

The total exergy of a system can be determined by using

$$b_{tot} = b_k + b_p + b_{ph} + b_{ch}, \qquad (1)$$

where b_k refers to the kinetic exergy, b_p to the potential exergy, b_{ph} to the physical exergy, and b_{ch} to the chemical exergy. In most applications that involves industrial processes, kinetic and potential exergy can be neglected (Dincer and Rosen, 2013), simplifying (1) to

$$b_{tot} = b_{ph} + b_{ch}. \qquad (2)$$

The calculated exergy can therefore describe both the physical state and the chemical features of the process. Chemical features which the physical exergy cannot adequately account for, i.e. a stream's physical properties may remain unchanged, however, a deviation in stream composition can be present.

3.1 Physical Exergy

The physical exergy characterisation of a system accounts for the mechanical exergy, which is associated with deviations in pressure, and the thermal exergy, which is associated with deviations in temperature (Tsatsaronis, 2007). The physical exergy of any given material stream present in a system is given by

$$b_{ph} = (h - h_0) - T_0(s - s_0), \qquad (3)$$

where h and s are the enthalpy and entropy values respectively of the stream at its initial thermodynamic state. h_0 and s_0 are the enthalpy and entropy values of the stream present at the reference environment. T_0 is the temperature of the reference environment. The enthalpy and entropy associated with the physical exergy in (3) can be calculated by using (4) and (5) respectively:

$$(h - h_0) = \int_{T_0}^{T} Cp \ dT, \qquad (4)$$

$$(s - s_0) = \int_{T_0}^{T} Cp/T \ dT - R \ln P/P_0. \qquad (5)$$

Cp is the heat capacity of the stream under consideration, R is the universal gas constant and P_0 is the pressure of the reference environment. The reference environment is defined as $T_0 = 25$ °C and $P_0 = 101.325$ kPa (Querol et al., 2012).

3.2 Chemical Exergy

Chemical exergy can be characterised into two parts, namely reactive exergy and non-reactive exergy. Reactive exergy is associated with any changes that arise because of chemical reactions, whereas non-reactive exergy is associated with any process which results in the change of a systems chemical concentration such as mixing, expansion, compression or separation (Tsatsaronis, 2007; Rivero et al., 2006). Therefore, the chemical exergy of a system plays a significant role whenever any chemical reactions, mixing or phase changes occur in a process (Dincer and Rosen, 2013). The most generic form used to express the chemical exergy of a substance is given by

$$b_{ch} = \sum x_{(i)} b_{ch(i)}^0, \qquad (6)$$

where $x_{(i)}$ is the mole fraction and $b_{ch(i)}^0$ is the standard molar chemical exergy of substance i (Querol et al., 2012). The standard chemical exergy of a substance varies for different phases. To take this into account, the total chemical exergy is calculated by the sum of the vapour and liquid phase exergy,

$$b_{ch} = \sum x_{(i)v} b_{ch(i)v}^0 + \sum x_{(i)l} b_{ch(i)l}^0. \qquad (7)$$

If the phase is not present in the stream the corresponding phase exergy is assumed to be zero.

For the accurate calculation of chemical exergy, the standard chemical exergy of the substance under consideration is required. Methods to calculate the standard chemical exergy for various substances has been extensively researched, computed and tabulated throughout the years. These sources include Szargut et al. (1988), Kotas (1995) and Rivero et al. (2006), to name but a few. Unfortunately, when applied to the components used in the TEP, the proposed methods or tabulated values cannot be directly used due to the unknown nature of these components. The only information pertaining to the unknown components that can be gained from the source code of the TEP are certain physical and thermodynamic properties, which include the components' molecular weight, heat capacities and liquid densities.

Research done by Gharagheizi and co-workers (Gharagheizi and Mehrpooya, 2007; Gharagheizi et al., 2014, 2018), indicated the possibility that a correlation could be made between certain properties of a substance and its standard chemical exergy. They developed two models based on the chemical structure of pure components and one based on the formation reaction of an organic compound related to the enthalpy and entropy of its constituent elements. Therefore, a study was conducted to see if a correlation could be established between the known physical and thermodynamic properties, and standard chemical exergy.

First, the standard chemical exergy and properties (as mentioned above), for known substances were gathered. As mentioned previously, the chemical exergy of a substance varies with regards to its phase, therefore the standard chemical exergy of a substance in liquid and vapour phase are considered separately. The tabulated values of 33 substances in the vapour phase and 59 substances in the liquid phase were obtained from literature (these values are given at the reference environment). Tabulated standard chemical exergies were found in Kotas (1995) and the physical properties from Yaws (1999)

For all TEP components in the vapour phase, their molecular weight, $MW_{(i)}$, and vapour heat capacity, $Cp_{v(i)}$, are available. Using the reference tabulated values, a linear regression analysis was done to find any correlation between these physical properties and the standard chemical exergy. The analysis yielded (8).

$$b_{ch(i)v}^0 = -510261 + 25667 Cp_{v(i)} + 13745 MW_{(i)} \qquad (8)$$

A comparison between the reference tabulated values and values calculated using (8) yielded a correlation coefficient of $R^2 = 0.92$, deeming it sufficient to calculate the standard chemical exergy of a substance in their vapour phase. The same procedure was followed for components in their liquid phase. For all TEP components in the liquid phase, their molecular weight, liquid heat capacity, $Cp_{l(i)}$, and liquid density, $\rho_{(i)}$, are available. A linear regression analysis between the standard chemical exergy and these physical properties resulted in (9).

$$\begin{aligned} b_{ch(i)l}^0 = 1537576 + 112.65 Cp_{l(i)} \\ + 49487 MW_{(i)} - 2973515 \rho_{(i)} \end{aligned} \qquad (9)$$

A correlation coefficient of $R^2 = 0.97$ was obtained when comparing the reference tabulated values and values estimated from (9), deeming it sufficient to calculate the standard chemical exergy for a substance in their liquid phase. For both these equations, the molecular weight is in g/mol, the heat capacities are in J/mol·K, and the liquid density in g/cm^3.

Equations (8) and (9) represent a new approach to calculating the standard chemical exergy of any component of which the appropriate physical and thermodynamic properties are known. Therefore, the standard chemical exergies of the TEP components A to G, for both the vapour and liquid phase, are calculated using (8) and (9) respectively, as shown in Table 1.

4. EXERGY-BASED FAULT DETECTION

To Calculate the exergy of any process stream, certain thermodynamic data should be available. These include

Table 1. Standard molar chemical exergy for
the TEP components.

Component	Vapour phase (J/mol)	Liquid phase (J/mol)
A	254 278	-
B	948 838	-
C	625 079	-
D	1 822 034	2 118 895
E	1 979 455	2 331 760
F	2 321 416	2 492 349
G	1 491 254	2 279 927
H	1 822 996	2 994 129

physical properties of process streams, chemical composition, as well as the enthalpy and entropy associated with these streams. With regards to the TEP, only data that could be directly extracted from the process without using any extra equations (beyond those already used for the exergy) or making any more assumptions beyond what the TEP already assumes, are used to show how exergy is applied. This data are not limited to the 41 process measurements or 12 manipulated variables and include underlying data used by the process simulation to calculate these measured and manipulated variables. After a thorough examination of the Simulink model of the TEP, seven streams were identified where all needed information could be obtained. The identified streams are indicated in Fig. 1. Therefore, 14 exergy variables are determined for the TEP, with physical and chemical exergy calculated for each of the seven considered streams.

The fault detection method compares the exergy data of the process under normal operating conditions with exergy data when faulty operating conditions are implemented. Initially the process was simulated at normal operating conditions (therefore no faults are present). The data obtained from the exergy characterisation step were then used to determine thresholds that will define the boundaries of faulty operations for the exergy variables. These thresholds are determined with a very simple yet effective method for fault detection, i.e. the Shewhart control chart.

The purpose of the Shewhart control chart is to monitor individual variables over a certain time period to determine if the variable remains within its normal boundaries. The boundaries used to monitor the variables consists of upper and lower fault detection control limits, which are computed from data associated with normal operating conditions (Montgomery, 2007). The upper and lower control limits for each exergy variable are computed by

$$UCL_j = \mu_j + k\sigma_j, \tag{10}$$

$$LCL_j = \mu_j - k\sigma_j, \tag{11}$$

where UCL_j and LCL_j are the upper and lower control limits of exergy variable j respectively. μ_j and σ_j is the mean value and standard deviation of exergy variable j respectively. k denotes the threshold distance from the mean value and typically a k value of 3 is used since this will account for almost 99.74% of all deviations in the data. Sample data are used to construct these limits and the k value is critical in minimizing false alarms as well as missed detections. This value can therefore change depending on the considered process (Chiang et al., 2000; Montgomery, 2007). For the purpose of testing the exergy-

based fault detection method, k values of 1, 1.5, 2, 2.5 and 3 are investigated.

Quantifying the extent to which the faults are detectable will be done by computing the fault detection metrics, i.e. the false alarm rate (FAR) and the missed detection rate (MDR). The false alarm rate, given by (12), quantifies the number of normal samples identified as a fault,

$$FAR = \frac{N_{N,F}}{N_N} \times 100. \tag{12}$$

$N_{N,F}$ is the number of normal samples identified as faults and N_N the total number of fault free samples. The FAR is determined from data associated with normal operating conditions. The missed detection rate, given by (13), quantifies the number of samples within a faulty dataset that are wrongly identified as being within the control limits,

$$MDR_j = \frac{N_{F,N}}{N_F} \times 100. \tag{13}$$

$N_{F,N}$ is the number of faults samples identified as normal and N_F the total number of fault samples. The MDR is only applied when a fault is considered.

5. RESULTS AND DISCUSSION

In this study, an exergy-based fault detection method is tested on the TEP. The data used to test this method consists of 21 datasets, one corresponds with the normal operating condition (NOC) and the remaining 20 datasets correspond to the 20 programmed TEP faults. All simulations started with no faults, with faults being introduced 1 hour into the simulation time. Each run had a simulation time of 25 hours. Each set contains 14 exergy variables and 500 samples. For the purpose of fault detection, the exergy variables associated with the 20 faults are compared to the upper and lower control limits determined for the corresponding exergy variable. Although the programmed TEP consists of control loops designed to return to normal operating conditions once a fault occurs, some instance of abnormal behaviour will be present after a fault is introduced and will persist for some time depending on the control structure. The exergy-based fault detection method will therefore be effective if these induced faults produce abnormal behaviour that violated the control limits. When two consecutive samples of any exergy variable violate these control limits, a fault is declared and therefore, deemed detectable (Amin et al., 2019). However, if none of the limits are violated and the exergy variables stay within these boundaries the assumption is that no fault is present.

Several faults can almost immediately be detected with the threshold limits. Since some or all of the exergy variables considered show a significant deviation from the normal operating data. Making these faults easily detectable by monitoring each exergy variable. An example of this is shown in Fig.2, where an immediate deviation from the normal operating data can be seen. Fig.2 shows the chemical exergy variable calculated for the reactor feed stream (stream 6) under NOC, when fault 2 occurs and when fault 14 occurs. It can be seen that the exergy variable starts to deviate when fault 2 is introduced and not long after the threshold limit is violated. For a k value

of 3, fault 2 has an MDR of 24%, decreasing to 9% and 6.5% for k values of 2 and 1 respectively.
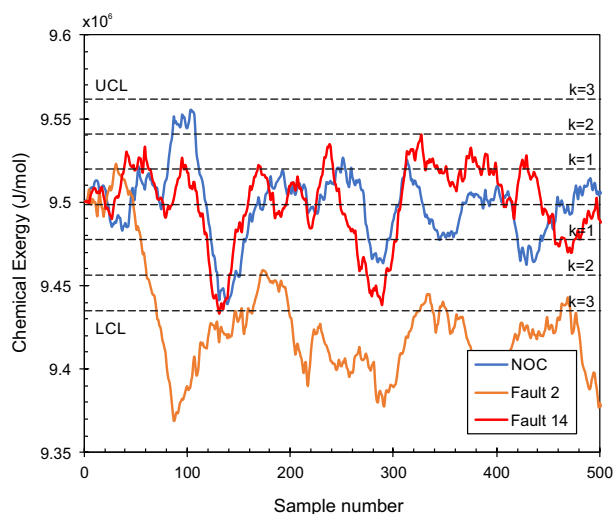
Fig. 2. The chemical exergy calculated for stream 6 under normal operating conditions and when faults 2 and 14 occurs.

Unfortunately, concerning fault 14 shown in Fig.2, no obvious deviation from normal data can be observed and the exergy variable falls well within the boundaries of the normal data. For a k value of 3, fault 14 has an MDR of 100% since no samples violate this threshold limit. This makes some faults hard to detect since no observable change in the mean and standard deviation can be observed. The MDR is slightly improved from 93% to 61% for k values of 2 and 1 respectively. However, as can be seen from Fig.2, even though the MDR values of the lower k values did improve, with these threshold limits normal operating data would also be flagged as faulty behaviour. This would not be ideal for the purpose of fault detection.

When investigating a fault detection method a trade-off is made between the FAR and MDR. Inevitably a decrease in one almost always results in the increase of the other. High FARs and low MDRs are associated with tight threshold limits, while if these threshold limits are too far apart it will result in low FARs and high MDRs (Chiang et al., 2000). This behaviour can clearly be seen in Table 2, where the threshold limits increase with every value of k, the FAR decreases and the MDR increases. The performance of this threshold method is therefore highly dependent on the selection of the k value.

Table 2. Fault detection metrices.

	$k = 1$	$k = 1.5$	$k = 2$	$k = 2.5$	$k = 3$
Average FAR %	37.4	19.2	8.36	3.43	0.71
Average MDR %	36.5	49.6	59.3	66.5	71.3
Faults detected	20	20	20	17	15

For all values of k, the exergy variables showed a certain deviation from the NOC. However, for the k value of 3, some faults had a limited effect on the exergy variables. Instances where the MDR value = 100% did occur, indicating that the exergy variables were not greatly affected by the considered fault. Because of this 5 faults were very difficult to detect, all having an average MDR value of above 96%. These were faults 4, 11, 14, 15 and

19. For a k value of 2.5, 17 of the 20 considered faults could be detected. In this case it was just faults 4, 11 and 14 that had very high MDR values, making them very difficult to detect. Therefore, from the data provided in Table 2 it was conclude that the best threshold limit for the exergy-based method was a k value of 2.5.

Table 3 shows the MDR values obtained for all exergy variables when the threshold limit was determined from a k value of 2.5. The smallest MDR value for all faults are shown in bold.

For faults 4, 11 and 14 very little deviation from the normal data could be observed. The lowest MDR values were found for the chemical exergy of stream 11 in all three fault cases. These faults all concerned some sort of change in the reactor cooling water temperature. From this it is seen that the exergy-based method had difficulty detecting these type of faults. Fault 19 also presented several high MDR values, with the lowest one being 69%. However overall the deviations that did occur could be distinguished from the NOC.
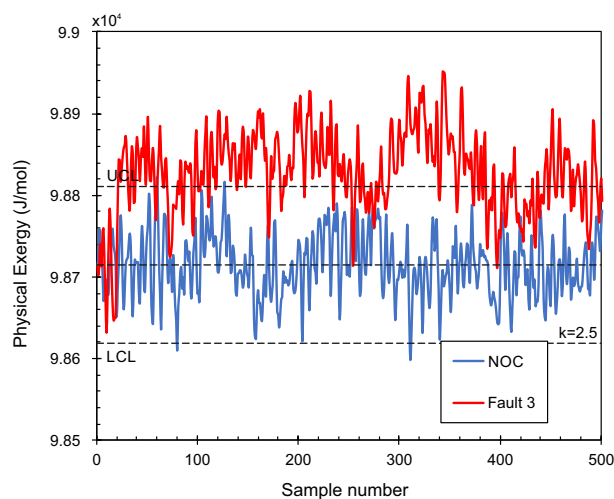
Fig. 3. Physical exergy of stream 6 for NOC and fault 3.

Faults 3, 9 and 15 are more often than not considered to be unobservable from the TEP data. Faults 3 and 9 are associated with a change in the temperature of stream 2, which is the feed stream of component D. Fault 15 is associated with a fault occurring with the condenser cooling water valve. Chiang et al. (2000), using a basic principle component analysis, declared very high MDR values for these faults and stated that no discernable change could be observed when comparing the variables associated with these faults with the NOC. Ammiche et al. (2018) reported fault 3 non detectable because the fault impact was very small.

In the case of the exergy-based method, the same trend could be seen for most exergy variables concerning fault 3 and 9. For faults 3 and 9 most exergy variables had a very high MDR value. However, every exergy variable is looked at separately and the fault is deemed detectable even if only one variable showed significant deviation. This is seen in the case of fault 3, where all but one exergy variable had fairly high MDR values. The variable in question was $b_{ph,1}$, which had an MDR value of 30%. When visually comparing the plots of the exergy variable

Table 3. Missed detection rates for the considered faults.

Fault	TEP Stream 6		TEP Stream 7		TEP Stream 8		TEP Stream 9		TEP Stream 10		TEP Stream 5		TEP Stream 11	
	$b_{ch,1}$	$b_{ph,1}$	$b_{ch,2}$	$b_{ph,2}$	$b_{ch,3}$	$b_{ph,3}$	$b_{ch,4}$	$b_{ph,4}$	$b_{ch,5}$	$b_{ph,5}$	$b_{ch,6}$	$b_{ph,6}$	$b_{ch,7}$	$b_{ph,7}$
1	56	46	57	65	57	84	57	84	53	70	16	**2**	50	13
2	15	37	15	**8**	46	44	46	44	27	25	58	15	54	12
3	94	**30**	94	94	94	99	94	99	93	96	98	90	84	90
4	91	99	91	97	92	99	92	99	86	97	99	96	**77**	95
5	65	79	**64**	77	**64**	88	**64**	88	68	81	94	74	80	72
6	5	3	6	2	6	5	6	5	**1**	5	14	4	2	10
7	45	62	45	53	45	86	45	86	51	67	81	51	69	**43**
8	28	44	27	**19**	28	67	28	67	39	48	69	26	43	26
9	84	**48**	85	90	84	97	84	97	88	94	97	90	66	89
10	89	84	87	96	88	96	88	96	85	95	98	**54**	79	62
11	96	94	96	96	96	97	96	97	86	95	98	95	**75**	95
12	26	21	27	25	25	23	25	23	26	**19**	66	23	59	25
13	36	37	35	**12**	35	43	35	43	19	28	55	19	17	22
14	95	96	96	89	96	97	96	97	93	97	97	96	**87**	98
15	91	96	90	94	91	99	91	99	84	95	98	89	**76**	90
16	88	90	88	96	89	98	89	98	93	97	99	**62**	90	73
17	81	79	79	86	81	89	81	89	**78**	85	98	88	**78**	92
18	15	19	**15**	25	**15**	41	**15**	41	17	22	36	22	23	25
19	92	95	93	98	93	97	93	97	84	97	98	96	**69**	99
20	80	61	79	94	80	**49**	80	**49**	86	59	98	88	98	94

with the NOC, all of the high MDR value variables showed little to no observable change. However, as can be observed in Fig.3, when the $b_{ph,1}$ of fault 3 is shown against the corresponding NOC, a definite deviation can be seen. This deviation in the exergy variable can be directly related to the fault that occurred, i.e. a change in temperature that would immediately influence the specific streams physical exergy. The same can be seen for fault 9, where the $b_{ph,1}$ had an MDR value of 48%. From this it is concluded that fault 3 and 9 could be detected with the exergy-based method, showing improvement over previously reported results.

For fault 15 on the other hand, the exergy-based method had a little more difficulty in detecting the fault with its lowest MDR value being 76%. However a deviation from normal data could still be observed, indicating the faults detectability with the exergy-based method.

Fault 6, which is associated with a loss in feed stream A, had the lowest average MDR value of 5%. All the exergy variables were greatly influenced by this fault. Such an observation is typical when it comes to fault detection of complex industrial processes since these processes usually have recycle streams. When a big enough fault occurs in such a process, the fault propagates throughout the process as time progress. This increases the difficulty of isolating the fault since no one variable can be isolated as the root cause. For the rest of the faults several, or in certain cases all, exergy variables were significantly affected by the occurring fault. These exergy variables showed significant deviations from normal data, making all of them detectable.

6. CONCLUSION

The results of this study suggest that an exergy-based fault detection method can be adequately applied to a dynamic industrial system. The basic exergy-based method presented here could detect 17 of the 20 considered faults. It could also detect faults 3 and 9, which previous methods have shown to be difficult if not impossible to detect. The exergy-based approach does seem to have advantages in regards to its interpretability, since the energy parameters can be directly correlated to the process, as well as in terms of specificity (extent to which faults are mistaken for normal behaviour or other faults). This is due to the fact that the different faults will influence and change the exergy variables in different ways, which can make it very effective if considered for fault isolation. This is significant for future studies, especially when considered as the basis of a hybrid fault detection technique. However in terms of its sensitivity (the extent to which faults are actually detected) some more work is required to improve this approach. Since only faults that have a significant impact on the exergy features show a satisfactory performance, future work will also include a sensitivity analysis to show which variables have the biggest effect on the exergy features. These exergy features can then be combined with other popular fault detection techniques to produce a hybrid approach. This will be done to investigate whether such a hybrid method could result in an overall better fault detection technique which could detect all considered faults. A direct comparison with other methods will also be done in future studies to aid with the development of a hybrid approach. A direct comparison can highlight where one method outshines another which in turn can assist with deciding which combination of methods will result in the superior hybrid method.

ACKNOWLEDGEMENTS

REFERENCES

Amin, M.T., Imtiaz, S., and Khan, F. (2018). Process system fault detection and diagnosis using a hybrid technique. *Chemical Engineering Science*, 189, 191–211.

Amin, M.T., Khan, F., and Imtiaz, S. (2019). Fault detection and pathway analysis using a dynamic bayesian network. *Chemical Engineering Science*, 195, 777–790.

Ammiche, M., Kouadri, A., and Bakdi, A. (2018). A combined monitoring scheme with fuzzy logic filter for plant-wide Tennessee Eastman process fault detection. *Chemical Engineering Science*, 187, 269–279.

Bouamama, B.O., Biswas, G., Loureiro, R., and Merzouki, R. (2014). Graphical methods for diagnosis of dynamic systems. *Annual reviews in control*, 38(2), 199–219.

Chen, Z., Zhang, K., Ding, S.X., Shardt, Y.A., and Hu, Z. (2016). Improved canonical correlation analysis-based fault detection methods for industrial processes. *Journal of Process Control*, 41, 26–34.

Chiang, L.H., Russell, E.L., and Braatz, R.D. (2000). *Fault detection and diagnosis in industrial systems*. Springer Science & Business Media.

Dincer, I. and Rosen, M.A. (2013). *Exergy: energy, environment and sustainable development*. Elsevier, 2nd edition.

Downs, J.J. and Vogel, E.F. (1993). A plant-wide industrial process control problem. *Computers & chemical engineering*, 17(3), 245–255.

Eslamloueyan, R. (2011). Designing a hierarchical neural network based on fuzzy clustering for fault diagnosis of the Tennessee Eastman process. *Applied soft computing*, 11(1), 1407–1415.

Ge, Z., Song, Z., and Gao, F. (2013). Review of recent research on data-based process monitoring. *Industrial & Engineering Chemistry Research*, 52(10), 3543–3562.

Gharagheizi, F., Ilani-Kashkouli, P., and Hedden, R.C. (2018). Standard molar chemical exergy: A new accurate model. *Energy*, 158, 924–935.

Gharagheizi, F., Ilani-Kashkouli, P., Mohammadi, A.H., and Ramjugernath, D. (2014). A group contribution method for determination of the standard molar chemical exergy of organic compounds. *Energy*, 70, 288–297.

Gharagheizi, F. and Mehrpooya, M. (2007). Prediction of standard chemical exergy by a three descriptors QSPR model. *Energy Conversion and Management*, 48(9), 2453–2460.

Greyling, S., Marais, H., van Schoor, G., and Uren, K.R. (2019). Application of exergy-based fault detection in a gas-to-liquids process plant. *Entropy*, 21(6), 565.

Guo, L. and Kang, J. (2015). A hybrid process monitoring and fault diagnosis approach for chemical plants. *International Journal of Chemical Engineering*, 2015.

Kotas, T. (1995). *The Exergy Method of Thermal Plant Analysis*. Butterworth-Heinemann.

Liao, L. and Köttig, F. (2016). A hybrid framework combining data-driven and model-based methods for system remaining useful life prediction. *Applied Soft Computing*, 44, 191–199.

Lyman, P.R. and Georgakis, C. (1995). Plant-wide control of the Tennessee Eastman problem. *Computers & chemical engineering*, 19(3), 321–331.

Marais, H., van Schoor, G., and Uren, K. (2019). The merits of exergy-based fault detection in petrochemical processes. *Journal of Process Control*, 74, 110–119.

Maurya, M.R., Rengaswamy, R., and Venkatasubramanian, V. (2007). A signed directed graph and qualitative trend analysis-based framework for incipient fault diagnosis. *Chemical Engineering Research and Design*, 85(10), 1407–1422.

Montgomery, D.C. (2007). *Introduction to statistical quality control*. John Wiley & Sons.

Querol, E., Gonzalez-Regueral, B., and Perez-Benedito, J.L. (2012). *Practical approach to exergy and thermoeconomic analyses of industrial processes*. Springer Science & Business Media.

Ragab, A., El-Koujok, M., Poulin, B., Amazouz, M., and Yacout, S. (2018). Fault diagnosis in industrial chemical processes using interpretable patterns based on logical analysis of data. *Expert Systems with Applications*, 95, 368–383.

Reis, M. and Gins, G. (2017). Industrial process monitoring in the big data/industry 4.0 era: From detection, to diagnosis, to prognosis. *Processes*, 5(3), 35.

Rivero, R., , and Garfias, M. (2006). Standard chemical exergy of elements updated. *Energy*, 31(15), 3310–3326.

Szargut, J., Morris, D., and Steward, F. (1988). *Energy analysis of thermal, chemical, and metallurgical processes*. Hemisphere Publishing, New York, NY.

Tidriri, K., Chatti, N., Verron, S., and Tiplica, T. (2018a). Model-based fault detection and diagnosis of complex chemical processes: A case study of the Tennessee Eastman process. *Proceedings of the Institution of Mechanical Engineers, Part I: Journal of Systems and Control Engineering*, 232(6), 742–760.

Tidriri, K., Tiplica, T., Chatti, N., and Verron, S. (2018b). A generic framework for decision fusion in fault detection and diagnosis. *Engineering Applications of Artificial Intelligence*, 71, 73–86.

Tsatsaronis, G. (2007). Definitions and nomenclature in exergy analysis and exergoeconomics. *Energy*, 32(4), 249–253.

Venkatasubramanian, V., Rengaswamy, R., and Kavuri, S.N. (2003a). A review of process fault detection and diagnosis: Part II: Qualitative models and search strategies. *Computers & chemical engineering*, 27(3), 313–326.

Venkatasubramanian, V., Rengaswamy, R., Yin, K., and Kavuri, S.N. (2003b). A review of process fault detection and diagnosis: Part I: Quantitative model-based methods. *Computers & chemical engineering*, 27(3), 293–311.

Wang, Y., Yang, H., Yuan, X., and Cao, Y. (2018). An improved bayesian network method for fault diagnosis. *IFAC-PapersOnLine*, 51(21), 341–346.

Wu, H. and Zhao, J. (2018). Deep convolutional neural network model based chemical process fault diagnosis. *Computers & chemical engineering*, 115, 185–197.

Yaws, C.L. (1999). *Chemical properties handbook*. McGraw-Hill,.

Yin, S., Ding, S.X., Haghani, A., Hao, H., and Zhang, P. (2012). A comparison study of basic data-driven fault diagnosis and process monitoring methods on the benchmark Tennessee Eastman process. *Journal of process control*, 22(9), 1567–1581.